Capacity Enhancement of Uni-directional In-band Full-Duplex Cellular Networks through Co-channel Interference Cancellation

Hyungsik Ju, Donghyuk Gwak, Sun-Ae Kim, Yuro Lee, and Tae-Joong Kim

As implementation of the in-band full duplex (IFD) transceiver becomes feasible, research interest is growing with respect to using IFD communication with cellular networks. However, the cellular network in which the IFD communication is applied inevitably suffers from an increase of the co-channel interference (CCI) due to IFD simultaneous transmission and reception. In this paper, we analyze the performance of a cellular network based on uni-directional IFD (UD-IFD) communication, wherein an IFD base station simultaneously supports downlink and uplink transmissions of half-duplex (HD) users. In addition, a multi-pair CCI cancellation (MP-CCIC) method combining CCIC and user pairing is proposed to improve the performance of the UD-IFD network. Simulation results showed that, compared to a conventional HD cellular network without using CCIC, capacity gain was not obtained in the UD-IFD cellular network. On the other hand, when applying the proposed MP-CCIC, the capacity of the UD-IFD cellular network greatly improved compared to that of an HD cellular network.

Keywords: CCI cancellation (CCIC), Cellular network, Co-channel interference (CCI), In-band full-duplex (IFD), Uni-directional IFD (UD-IFD), User pairing.

I. Introduction

In-band full-duplex (IFD) communication has recently received considerable attention because the simultaneous transmission and reception of signals in the same frequency band led by IFD has the potential to double the link capacity compared to conventional half-duplex (HD) communications. This capacity improvement is predicated on the complete elimination of self-interference (SI), which is the transmitted signal of a node received by the node itself. It thus severely interferes with the desired received signal. Therefore, among the various issues related to IFD, SI cancellation (SIC) has been the most intensively studied. In this regard, many SIC algorithms that enable IFD communication have been proposed [1]–[4]. In particular, the practical feasibility of IFD communication has been verified through a proof-of-concept, which showed that the power of the residual SI after SIC can be reduced up to the level of the background noise [1], [2].

Research attention has now led to the application of IFD technology to cellular networks, and many related studies have been published [5]. In a cellular network, the application of IFD enables the simultaneous support of a downlink (DL) and an uplink (UL) within the same frequency band, whereby the network performance is expected to improve. When IFD is applied to a cellular network, there are two typical models for simultaneous DL and UL support. The first is a *bi-directional IFD* (BD-IFD) model, in which a base station (BS) operating in IFD

Manuscript received Apr. 17, 2017; revised Aug. 21, 2017; accepted Sept. 20, 2017.

Hyungsik Ju (corresponding author, jugun@etri.re.kr), Donghyuk Gwak (gwakdh@etri.re.kr), Sun-Ae Kim (sun0811@etri.re.kr), Yuro Lee (eyurolee@etri.re.kr), and Tae-Joong Kim (aisma@etri.re.kr) are with the 5G Giga Service Research Laboratory, ETRI, Daejeon, Rep. of Korea.

supports both the DL and UL of the user equipment (UE) that also operates in IFD. The other is a *uni-directional IFD* (UD-IFD) model, in which an IFD BS simultaneously supports DL/UL transmissions to/from different HD UEs, respectively.

When IFD is applied to cellular networks, however, another inherent problem arises in addition to SI, that is, an increase in co-channel interference (CCI) [6]. This increase in CCI originates from the fact that the IFD operation in a cellular network makes a DL and UL simultaneously active. In a conventional cellular network based on HD communications (herein, an HD cellular network), CCI entering from other cells (in other words, inter-cell CCI) occurs because the DL/UL transmission of a cell interferes with the DL/UL reception of other cells.

In a cellular network based on IFD communication, however, additional inter-cell CCI occurs in addition to that occurring in an HD cellular network because both DL and UL transmissions of a cell interfere with both UL and DL receptions of the other cells. In an IFD cellular network applying the UD-IFD model (herein, UD-IFD cellular networks), another type of CCI, so-called intra-cell CCI, also occurs because a UL transmission in a cell interferes with the DL reception within the same cell. Considering the increase in CCI, the performance of IFD cellular networks was studied in [6]–[13].

The performance of an IFD cellular network applying the BD-IFD model (herein, BD-IFD cellular network) has mainly been analyzed using stochastic geometry frameworks [6]–[9]. In [6] to [8], the performance of a BD-IFD cellular network was analyzed by assuming perfect SIC on both BS and UE sides, where each IFD BS and IFD UE pair is modeled through a bipolar point process [6], [7] and a Thomas cluster point process [8]. In [9], the performance of a BD-IFD cellular network was studied in the presence of residual SI at the BSs and UEs. The results in [6]–[9] showed that the performance of a cellular network can be significantly improved by adopting BD-IFD communication between the IFD BS and IFD UE in each cell. In addition, the performance of a UD-IFD cellular network was investigated in [10]–[13]. In [10] and [11], the performance of a UD-IFD cellular network in conjunction with scheduling and transmit power allocating was investigated through simulations.

Furthermore, the DL and UL performances in a UD-IFD cellular network were experimentally evaluated using the 3rd Generation Partnership Project (3GPP) Long Term Evolution (LTE) Release 9 test bed [12]. Furthermore, the cell throughput of a UD-IFD cellular network in the presence of residual SI at the IFD BSs was analyzed by utilizing a homogeneous Poisson point process framework [13]. The results of these studies showed that, compared to that of an HD cellular network, the performance of a UD-IFD cellular network was not enhanced without control of the CCI. In particular, the presence of intra-cell CCI had a much more significant impact on the performance than the increase in the inter-cell CCI. Therefore, it is necessary to control the intra-cell CCI in UD-IFD cellular networks to achieve a performance gain originating from the employment of an IFD operation.

It is worth noting that, despite the fact that degraded performance from CCI is more serious, the UD-IFD model has received more attention than the BD-IFD model for deployment in cellular networks because of the inefficiency and difficulties in installing an IFD transceiver in the UE, as well as the potential for backward compatibility. Provided that the CCI (particularly, intra-cell CCI) is properly managed at a DL UE, the UD-IFD model can provide a more immediate and promising application of IFD technology to a cellular network. In this paper, we therefore focus on a UD-IFD cellular network and study the effects of applying CCI cancellation (CCIC) at a DL UE for removal of intra-cell CCI on the overall capacity.

Meanwhile, CCIC schemes applied at a DL UE to cancel the intra-cell CCI have been studied [14]–[17]. In [14], a CCIC method that utilizes a side-channel was proposed. Using this method, the information of the channel between a DL UE and the interfering UL UE is sent to the BS. In addition, the effects of channel state information at the transmitter (CSIT) on the CCIC performance and the corresponding throughput of a UD-IFD cellular network have been analyzed [15]. Finally, opportunistic CCIC schemes based on the received power of intra-cell CCI at a DL UE have been studied [16], [17].

In this paper, we describe the performance of a UD-IFD cellular network based on simulations using the methodology from [18]. We then propose a CCIC scheme for a DL UE that removes CCI based on the received power. Although the proposed CCIC method is mainly intended for eliminating intra-cell CCI, the removal range of CCI is not limited to intra-cell CCI; it also covers inter-cell CCI in certain cases. In addition, the proposed CCIC scheme does not utilize a side channel because doing so requires an additional frequency band and thus degrades the spectral efficiency. We first evaluate and compare the capacity of an HD cellular network and a UD-IFD cellular network with/without the CCIC scheme in the presence of a DL UE and UL UE pair in each cell. We then extend our scope to an environment in which multiple pairs of DL and UL UEs are distributed in each cell, and we propose a multi-pair CCIC (MP-CCIC) algorithm in conjunction

https://doi.org/10.4218/etrij.2017-0093

with a new method of DL UE and UL UE pairing based on the location information. Finally, we show the capacity enhancement resulting from the proposed MP-CCIC.

The remainder of this paper is organized as follows. Section II presents a UD-IFD cellular network model and the simulation parameters used later in this paper. Section III evaluates the effects of CCIC on the capacity of a UD-IFD cellular network in the presence of a single DL UE and UL UE pair in each cell. In Section IV, we describe the MP-CCIC algorithm proposed for a UD-IFD cellular network, and we show the performance enhancement achieved by its application. Finally, Section V provides concluding remarks on this research.

II. System Model

In this section, we address the UD-IFD cellular network model and the simulation parameters used later in this paper.

1. UD-IFD Cellular Network Model

Figure 1 shows the UD-IFD cellular network model consisting of one IFD BS, one HD DL UE, and one HD UL UE per cell. In each cell of the UD-IFD cellular network, the IFD BS transmits a DL signal to the DL UE while simultaneously receiving the UL signal transmitted by the UL UE. Because the DL and UL transmissions in each cell are simultaneously conducted, the cell capacity of the UD-IFD cellular network can be ideally increased up to twofold.

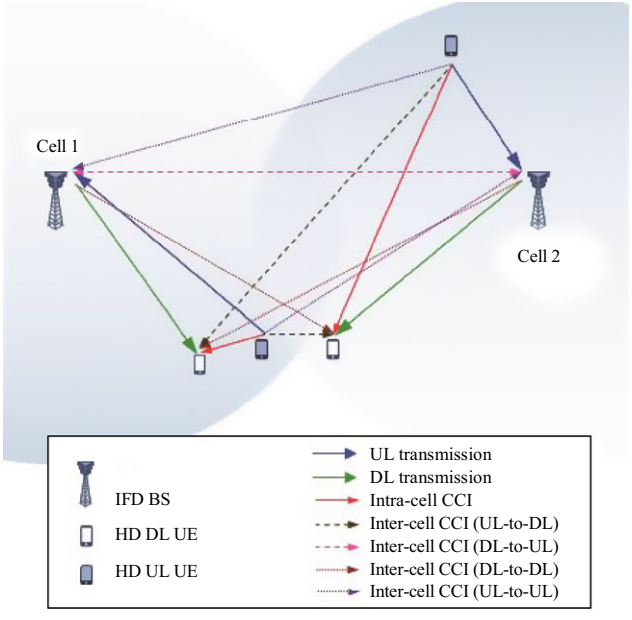

Fig. 1. UD-IFD cellular network model and CCI description.

In the UD-IFD cellular network, however, CCI inherently increases compared to a conventional HD cellular network because DL and UL are simultaneously active. Figure 1 describes the CCI occurring in a UD-IFD cellular network. In a conventional HD cellular network in which the transmissions in the DL and UL are separated in time or frequency, there are two types of inter-cell CCI—*DL-to-DL* and *UL-to-UL* CCI— caused by a DL/UL transmission of a cell interfering with the DL/UL reception of the adjacent cells. In a UD-IFD cellular network, in addition to the aforementioned DL-to-DL and UL-to-UL CCI, there are two more types of inter-cell CCI occurring based on the feature in which both DL and UL are simultaneously active—that is, *DL-to-UL* and *UL-to-DL* CCI—caused by the DL/UL transmission of a cell interfering with the UL/DL reception of the adjacent cells. In particular, simultaneous transmissions in the DL and UL by a BS and UL UE in the same cell, respectively, cause *intra-cell CCI* in the reception of the DL signal of the DL UE in the same cell. In general, it is known that intra-cell CCI has a greater effect on the performance degradation in a UD-IFD cellular network than inter-cell CCI. Depending on the location of the UE, however, inter-cell CCI may affect the DL reception of the DL UE more significantly than intra-cell CCI. As shown in Fig. 1, for example, the performance of the DL UE in cell 2 is more significantly affected by the inter-cell UL-to-DL CCI caused by the UL UE in cell 1 than the intra-cell CCI caused by the UL UE in cell 2.

2. Simulation Environments

In this subsection, we address the simulation environment considered throughout this paper, which is mainly based on the *multi-cell macro-pico scenario* defined in [18]. The simulation parameters used later in this paper are summarized in Table 1.

Macro-cell base stations (MBSs) are deployed following a typical 19-cell and three-sectored hexagonal system layout. In addition, four pico-cell base stations (PBSs) equipped with a single-antenna IFD transceiver are randomly deployed on each sector of the macro-cells. In each pico-cell, there are K DL UEs and K UL UEs constituting K UE pairs, all of which have a single antenna and operate in HD. An IFD PBS and pairs of HD UEs in each pico-cell communicate following the UD-IFD model. The SI can be eliminated such that the power of the residual SI after SIC is applied can be reduced sufficiently close to that of the background noise [1], [2]. Accordingly, it is assumed, without loss of generality, that the SIC at each PBS is perfect. To further focus on the impact of CCI

Table 1. Simulation parameters.

Parameters		Description and value	
Scenario		Multi-cell macro-pico scenario [18]	
System bandwidth		10 MHz	
Carrier frequency		2 GHz	
Inter-site distance		500 m	
Macro deployment		Hexagonal system layout with 7 cells and 3 sectors/cell	
Pico deployment		40 m radios, random deployment	
Pico-cells per sector		4	
UEs per pico-cell		Uniformly dropped around PBS within 40 m	
Min. distance b/w pico-cells		40 m	
Min. distance b/w PBS and MBS		75 m	
Min. distance b/w PBS and UE		10 m	
PBS antenna pattern		2D, omni-directional	
PBS antenna gain		5 dBi	
UE antenna gain		0 dBi	
PBS noise figure		13 dBi	
UE noise figure		9 dBi	
Max. PBS TX power		24 dBi	
UE power class		23 dBi	
Shadowing standard deviation	b/w PBSs	6 dB	
	b/w PBS and UE	LOS	3 dB
		NLOS	4 dB
Shadowing	b/w PBSs	0.5	
Correlation	b/w PBS and UE	LOS	0
		NLOS	0

and CCIC on a UD-IFD network, the MBSs are furthermore assumed to be inactive. Finally, the performance of the DL and UL transmissions of the UD-IFD network configured in each pico-cell is measured only in the macro-cell located at the center.

The wireless channels between different PBSs, between a PBS and UE, and between different UEs are all characterized by only large-scale fading (in other words, signal power attenuation owing to distance-dependent path loss and shadowing), whereas small-scale fading is not considered because resource allocation based on small-scale channel fading is beyond the scope of this paper. For more detailed models of wireless channels, refer to [18].

In this network, the wireless channels are assumed to follow quasi-static block fading, where all channels remain constant during a specific block duration. Accordingly, we consider a frame-based block transmission in which one transmission block consists of K time slots (in other words, subframes), and each time slot is allocated to a DL UE and UL UE pair for their respective DL reception and UL transmission.

III. CCIC in UD-IFD Cellular Network

As addressed in Section II, a DL UE in a UD-IFD cellular network is affected not only by the inter-cell CCI, but also by the intra-cell CCI. Intuitively, the intra-cell CCI received by a DL UE is minimized when the interfering UL UE in the same cell is located on the opposite side of the cell from the location of the DL UE with the maximum distance. However, it is difficult to guarantee that the UL UE paired with the DL UE will be located on the opposite side of the cell. Furthermore, the UL UE may be located close to the DL UE in adjacent cells in this case, which may cause a stronger inter-cell CCI to the DL reception of the adjacent cells. Therefore, it is difficult to expect a significant performance improvement of the UD-IFD cellular networks with a UE pairing strategy that simply selects the UL UE located on the opposite side of the DL UE in each cell.

Alternatively, another way to improve the DL performance of a UD-IFD cellular network is removing the CCI received by the DL UE. It is worth noting that, depending on the relative positions and distances between a DL UE and interfering UL UEs, it is more likely that an order exists in the received powers of the CCI at the DL UE. In this case, a DL UE can therefore sequentially decode and restore the CCI from the CCI with the largest received power—and then remove it from the received signal [19]—without discriminating between the intra-cell and inter-cell CCI.

At a DL UE, the decodability of the CCI with the largest received power is determined by evaluating its signal-to-interference-plus-noise ratio (SINR) when all remaining signals (including the desired DL signal) are regarded as noise, and then comparing the SINR with a pre-determined value, γ. By sorting all CCI received by a DL UE in descending order by their received power, the ith strongest CCI at the DL UE can be considered decoded and restored if

$$\frac{|h_{\mathrm{U},i}|^2 P_{\mathrm{U},i}}{|h_{\mathrm{D}}|^2 P_{\mathrm{D}} + \sum_{j=i+1}^{N} |h_{\mathrm{U},j}|^2 P_{\mathrm{U},j} + I_{\mathrm{D}} + \sigma_{\mathrm{UE}}^2} \geq \gamma, \qquad (1)$$

where N denotes the total number of interfering UL UEs that cause CCI to the DL UE. In addition, P_{D} and h_{D}

https://doi.org/10.4218/etrij.2017-0093

represent the transmit powers of the BS by which the DL UE is supported and the channel through which the desired DL signal to the DL UE passes, respectively. Furthermore, $h_{U,i}$ and $P_{U,i}$ represent the transmit power of the UL UE that causes the ith strongest UL CCI to the DL UE (including both intra-cell and inter-cell UL-to-DL CCI) and the channel through which the ith strongest UL CCI passes, respectively. Finally, I_D and σ_{UE}^2 denote the aggregated CCI caused by DL transmissions of BSs in the neighboring cells and the receiver noise at the UE, respectively. It is assumed in (1) that, if the ith strongest UL CCI among the intra-cell CCI and inter-cell UL-to-DL CCI can be removed, all the first through the $(i-1)$th strongest UL CCI are assumed to be decoded and already removed. For this, it is assumed that $h_{U,1}, h_{U,2}, \ldots, h_{U,i-1}$ are perfectly known by the DL UE. Furthermore, the CCIC method with (1) only removes the intra-cell CCI and inter-cell UL-to-DL CCI. This is because, at a DL UE, the received power of the inter-cell DL-to-DL CCI is generally less than that of the desired DL signal transmitted by the BS in the cell to which the DL UE belongs. Therefore, DL-to-DL CCI is neither decoded nor removed from the received signal at the DL UE, and I_D is thus regarded as background noise.

It is worth noting that the CCIC method with (1) can be applied independently at each DL UE. Therefore, UL transmissions are not affected by the application of this CCIC method, and the corresponding UL performance remains the same regardless of the employment of this CCIC method.

Figure 2 shows the cumulative distribution functions (CDFs) of the DL and UL capacities in an HD cellular network and UD-IFD cellular network, which are evaluated through simulations using the parameters defined in Table 1. The results are obtained in the presence of one DL UE and UL UE pair in each pico-cell. The figure also shows the effect of adopting CCIC with (1) on the DL capacity of a UD-IFD cellular network according to various values of γ. For comparison, the DL capacity of an IFD cellular network in which there is no intra-cell CCI is also included.

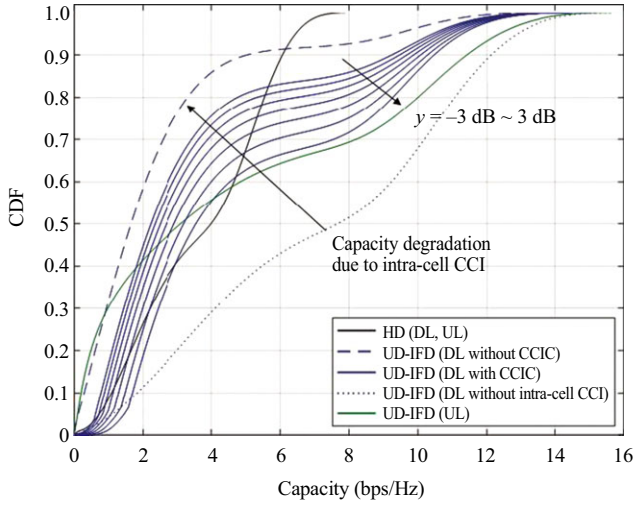

Fig. 2. CDF of DL capacity with/without CCIC.

As shown in the figure, the presence of intra-cell CCI severely degrades the DL capacity of a UD-IFD cellular network compared to the counterpart without intra-cell CCI. Even when compared with that of an HD cellular network, the DL capacity of a UD-IFD cellular network is degraded without the use of CCIC. However, the application of CCIC with (1) improves the DL capacity of a UD-IFD cellular network, whereas the UL capacity remains the same. The enhancement of the DL capacity by applying CCIC at a DL UE is clearly observed even when γ = 3 dB. Nonetheless, the DL capacity of a UD-IFD cellular network even with the CCIC is observed to be much poorer than that without intra-cell CCI. This implies that CCIC applied in the DL of a UD-IFD cellular network cannot completely remove the effects of intra-cell CCI on the DL performance.

Table 2 shows the increments of the average DL and sum capacities in a UD-IFD cellular network compared to those of an HD cellular network. Note that the UL capacity of a UD-IFD cellular network is not affected by the application of CCIC, and thus the corresponding UL capacity increment over an HD cellular network is observed to be 28.52% regardless of the CCIC threshold value γ.

Compared with an HD cellular network, the results show that the capacity increase in the UD-IFD network is not large, even when the CCIC is applied. When there is

Table 2. Increment of average DL and sum capacity of UD-IFD with CCIC over HD.

CCIC threshold (γ)	Increment (%, DL)	Increment (%, sum)
No CCIC	−34.86	−3.00
3 dB	−8.45	10.17
2 dB	−3.22	12.77
1 dB	2.89	15.88
0 dB	9.88	19.31
–1 dB	18.25	23.45
–2 dB	27.86	28.25
–3 dB	38.40	33.61
No intra-cell CCI	94.66	61.63

no intra-cell CCI, the increase in average DL capacity is 94.66%, which is close to the expected 100% capacity enhancement when IFD is applied in a cellular network. In the presence of intra-cell CCI, however, the DL capacity of a UD-IFD cellular network is considerably degraded compared to that of an HD cellular network if CCIC is not employed, or if it is applied with a γ larger than 2 dB. Furthermore, the increase in the DL capacity of a UD-IFD network is only 9.88% when γ is 0 dB, and a capacity gain of 40% can be expected if γ is less than -3 dB. On the other hand, the increase in the average sum capacity is observed to be 12.77%, 19.31%, and 28.25% when γ is 2 dB, 0 dB, and -2 dB, respectively, which are larger values than those of the DL capacity owing to the increase in UL capacity.

IV. Multi-pair CCIC in UD-IFD Cellular Networks

As addressed in Section III, it is difficult to effectively improve the DL capacity of a UD-IFD cellular network through CCIC when there is only one DL UE and UL UE pair in each cell. This is because the location of the UL UE must be sufficiently close to the location of the DL UE for effective CCIC; thus, the location of the UL UE to improve the DL capacity through the application of CCIC is very limited. In the presence of multiple DL UE and UL UE pairs, however, the CCIC performance can be enhanced owing to an increase in the degree-of-freedom in selecting a UL UE paired with a DL UE. In this section, we propose a CCIC mechanism for a UD-IFD cellular network that is suitable for a case with multiple DL UE and UL UE pairs, which is referred to as *multi-pair CCIC* (MP-CCIC). For convenience, CCIC in the presence of a single DL UE and UL UE pair in each cell is referred to as single-pair CCIC (SP-CCIC) later herein.

The proposed MP-CCIC consists of a user pairing based on a guard zone (GZ) and CCIC. The GZ is utilized to secure a sufficiently close distance between a paired DL UE and UL UE, considering the fact that the closer the DL UE and the UL UE are, the more advantageous it is to the CCIC. The user pairing associated with MP-SCCIC is intended to have as many UL UEs as possible located within the GZs of the DL UEs to minimize the number of DL UEs that are affected by the intra-cell CCI. Note that, after the user pairing is completed, the CCIC at each DL UE is applied in the same way as presented in the previous section. Therefore, a description of CCIC is omitted in this section for brevity; only the user pairing method is described.

1. GZ-Based User Pairing for MP-CCIC

In the presence of K DL UEs and K UL UEs in each cell, the proposed user pairing algorithm is performed by the BS to select the UL UE paired with each DL UE so that as many UL UEs as possible are located in the GZ of their associated DL UEs. The BS is assumed to have the location information of all DL and UL UEs and to utilize the information for UE pairing. After the pairing between the DL and UL UEs is completed, each UE pair is then assigned to each of the K time slots in a transmission block.

Based on the location information of the UEs, the BS first sets a circle of a given radius R around the position of a DL UE as the GZ of the DL UE, where the value of R is assumed to be a pre-determined constant. The distance between each DL UE and UL UE in a cell is saved in matrix $\mathbf{D}$, where $\mathbf{D}(i, j)$, the element of $\mathbf{D}$ on the ith row and jth column, denotes the distance between the ith DL UE and jth UL UE in the cell. In addition, a condition matrix denoted by $\mathbf{C}$ is defined, where the element of $\mathbf{C}$ on the ith row and jth column is initially given by

$$C(i,j) = \begin{cases} 1, & \text{if } D(i,j) \le R, \\ 0, & \text{otherwise.} \end{cases} \tag{2}$$

Each DL UE and UL UE pair that is assigned to each time slot is iteratively determined by updating $\mathbf{C}$ and $\mathbf{D}$. At the tth iteration, $\forall t = 1, 2, \ldots, K$, and we first obtain ω_t, which is given by

$$\omega_t = \sum_{i=1}^{K} \sum_{j=1}^{K} C(i,j). \tag{3}$$

Note that, if $\omega_t = 0$, there is no UL UE belonging to a GZ of any DL UE. Otherwise, if $\omega_t > 0$, there exists at least one UL UE that is located in a GZ of at least one DL UE. The selection of a DL UE and UL UE pair during the tth iteration is different for cases with $\omega_t = 0$ and $\omega_t > 0$.

When $\omega_t > 0$, we first choose a set of DL UEs, each of which has at least one UL UE in its respective GZ. Among them, the DL UE that has the smallest number of UL UEs in its GZ is selected as the active DL UE. A UL UE to be paired with the active DL UE is then selected. To this end, we define $\alpha_t(i)$, $i = 1, 2, \ldots, K$, as follows:

$$\alpha_t(i) = \begin{cases} \infty, & \text{if } \theta_t(i) = 0, \\ \theta_t(i), & \text{if } \theta_t(i) \neq 0, \end{cases} \tag{4}$$

where $\theta_t(i)$ denotes the sum of the elements in the ith row of $\mathbf{C}$ given by

$$\theta_t(i) = \sum_{j=1}^{K} C(i,j). \tag{5}$$

https://doi.org/10.4218/etrij.2017-0093

Note that $\theta_t(i)$ in (5) represents the number of UL UEs that lie in the GZ of the ith DL UE. Then, the d_tth DL UE is selected to be the active DL UE, where d_t is given by

$$d_t = \arg\min \left[\alpha_t(1), \alpha_t(2), \ldots, \alpha_t(K)\right]^T. \quad (6)$$

If there exist i and j, $i \neq j$, where $\alpha_t(i) = \alpha_t(j)$ holds, d_t can be determined to be either $d_t = i$ or $d_t = j$ (the selection of $d_t = i$ or $d_t = j$ does not affect the performance of the proposed user pairing algorithm).

To select the UL UE to be paired with the d_tth DL UE, we define two vectors—$\boldsymbol{\beta}_t = [\beta_t(1), \beta_t(2), \ldots, \beta_t(K)]$ and $\boldsymbol{\delta}_t = [\delta_t(1), \delta_t(2), \ldots, \delta_t(K)]$—where $\boldsymbol{\beta}_t$ and $\boldsymbol{\delta}_t$ represent the d_tth row vectors of **C** and **D** during the tth iteration, respectively. Furthermore, we define two other vectors—$\boldsymbol{\zeta}_t = [\zeta_t(1), \zeta_t(2), \ldots, \zeta_t(K)]$ and $\boldsymbol{\sigma}_t = [\sigma_t(1), \sigma_t(2), \ldots, \sigma_t(K)]$—where

$$\zeta_t(i) = \begin{cases} \infty, & \text{if } \beta_t(i) = 0, \\ \beta_t(i), & \text{if } \beta_t(i) \neq 0, \end{cases} \quad 1 \le i \le K, \quad (7)$$

$$\sigma_t(i) = \zeta_t(i)\delta_t(i), 1 \le i \le K. \quad (8)$$

Then, the u_tth UL UE is selected to be the pair of the d_tth DL UE, with u_t given by

$$u_t = \arg\min \left[\sigma_t(1), \sigma_t(2), \ldots, \sigma_t(K)\right]^T. \quad (9)$$

In the case in which there exist i and j, $i \neq j$, where $\min [\sigma_t(1), \ldots, \sigma_t(K)] = \sigma_t(i) = \sigma_t(j)$. We set $u_t = i$ if $D(d_t, i) > D(d_t, j)$ and vice versa. This is because the UL UE that is further from the d_tth DL UE is more likely to belong to the GZ of another DL UE.

After both d_t and u_t are determined, **C** is updated for the next iteration as:

$$C(d_t, j) = 0, \forall j = 1, 2, \ldots, K, \quad (10)$$

$$C(i, u_t) = 0, \forall i = 1, 2, \ldots, K. \quad (11)$$

The processes in (3) through (11) are then repeated while $\omega_t > 0$.

When $\omega_t = 0$, on the other hand, the values of d_t and u_t are determined based on **D**. We first set the elements of **D** as:

$$D(d_\tau, j) = 0, \forall \tau = 1, 2, \ldots, t-1, \quad (12)$$

$$D(i, u_\tau) = 0, \forall \tau = 1, 2, \ldots, t-1. \quad (13)$$

Then, d_t and u_t are determined, respectively, as

$$(d_t, u_t) = \arg\max_{i,j} D(i, j). \quad (14)$$

The processes in (3) and (10) through (14) are repeated until $t = K$. The proposed GZ-based user-pairing algorithm for the MP-CCIC addressed above is summarized in Algorithm 1.

Algorithm 1. Pseudo code for the proposed user pairing algorithm.

$D(i,j)$ = distance b/w ith DL UE & jth UL UE, $\forall i, j = 1, \ldots, K$

$C(i,j) = \begin{cases} 1, \text{ if } D(i,j) \le R, \\ 0, \text{ otherwise,} \end{cases} \forall i, j = 1, \ldots, K$

for $1 \le t \le K$

  $\omega_t = \sum_{i=1}^{K} \sum_{j=1}^{K} C(i,j)$

  if $\omega_t > 0$

    $\theta_t(i) = \sum_{j=1}^{K} C(i,j), \ \forall i = 1, \ldots, K$

    $\alpha_t(i) = \begin{cases} \infty, & \text{if } \theta_t(i) = 0, \\ \theta_t(i), & \text{if } \theta_t(i) \neq 0, \end{cases} \forall i = 1, \ldots, K$

    $d_t = \arg\min_i \left[\alpha_t(1), \alpha_t(2), \ldots, \alpha_t(K)\right]$

    $\beta_t(i) = C(d_t, i), \forall i = 1, \ldots, K$

    $\delta_t(i) = D(d_t, i), \forall i = 1, \ldots, K$

    $\zeta_t(i) = \begin{cases} \infty, & \text{if } \beta_t(i) = 0, \\ \beta_t(i), & \text{if } \beta_t(i) \neq 0, \end{cases} \forall i = 1, \ldots, K$

    $\sigma_t(i) = \delta_t(i)\zeta_t(i), \forall i = 1, \ldots, K$

    if $\arg\min_i \left[\sigma_t(1), \sigma_t(2), \ldots, \sigma_t(K)\right]$ is unique

      $u_t = \arg\min_i \left[\sigma_t(1), \sigma_t(2), \ldots, \sigma_t(K)\right]$

    else

      find $i_1, \ldots, i_M$ where $\min\left[\sigma_t(1), \ldots, \sigma_t(K)\right] = \sigma_t(i_1) = \cdots = \sigma_t(i_M)$

      $u_t = \arg\min_{i_m} \left[D(d_t, i_1), \ldots, D(d_t, i_M)\right]$

    end

    $C(d_t, j) = 0, \ \forall j = 1, \ldots, K$

    $C(i, u_t) = 0, \ \forall i = 1, \ldots, K$

  else

    $D(d_\tau, j) = 0, \ \forall \tau = 1, \ldots, t-1, \ \forall j = 1, \ldots, K$

    $D(i, u_\tau) = 0, \ \forall \tau = 1, \ldots, t-1, \ \forall i = 1, \ldots, K$

    $(d_\tau, u_\tau) = \arg\min_{i,j} D(i,j)$

  end

end

Figure 3 shows an example of the proposed user-pairing algorithm in a UD-IFD cellular network with $K = 7$. In this example, *DL UEs and UL UEs are paired in the order of* (D_4, U_1) → (D_1, U_5) → (D_2, U_6) → (D_5, U_2) → (D_6, U_3) → (D_3, U_4) → (D_7, U_7) in each iteration. They are then allocated to the first through seventh time slots, respectively. Here, D_4, D_1, D_2, D_5, and D_6, which have at least one UL UE in their respective GZs, are paired first with one of the UL UEs in their respective GZs, in other words, U_1, U_5, U_6, U_2, and U_3, respectively. Then, D_3 and D_7, which have no UL UEs in their GZs, are paired with the remaining UL UEs, U_4 and U_7, respectively.

On the other hand, D_1, D_2, D_4, D_5, and D_6 apply CCIC to remove the intra-cell UL CCI that is introduced from the transmissions of U_5, U_6, U_1, U_2, and U_3, respectively.

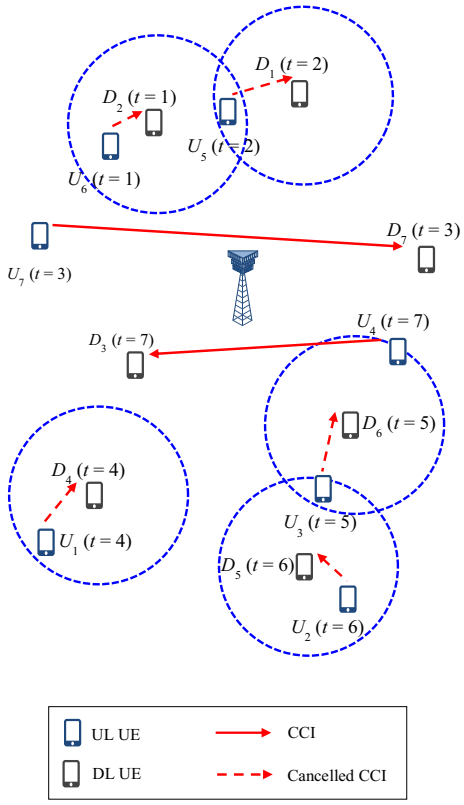

Fig. 3. Example of user scheduling for MP-SCCIC.

D_3 and D_7 do not apply CCIC because it is likely that the received power of their respective intra-cell CCI is not sufficiently large to decode it. Therefore, the DL receptions of D_3 and D_7 are affected by the intra-cell CCI caused by the UL transmissions of U_7 and U_3, respectively, whereas the DL receptions of other DL UEs are free from the intra-cell CCI.

Note that in this example, U_5 is located in the GZs of both D_1 and D_2. In this case, U_5 is paired with D_1 instead of D_2 to make both D_1 and D_2 apply SCCIC (if is U_5 paired with D_2, then D_1 cannot apply CCIC because there is no UL UE in its GZ after D_2 and U_5 are paired). In addition, U_4 is paired with D_3 instead of D_6 because, although both U_3 and U_4 are located in the GZ of D_6, it is more advantageous for D_6 to apply CCIC when it is paired with U_3 rather than U_4. After D_6 and U_3 are paired, U_4 does not belong to the GZ of any DL UE and is thus paired with D_3, which has no UL UE in its GZ and is farther from U_4 than D_7.

2. Performance of MP-CCIC

Figure 4 shows the percentage of DL UEs in the UD-IFD cellular network that are free from intra-cell CCI after SP-CCIC and MP-CCIC are applied. The results are obtained through simulations with the parameters defined

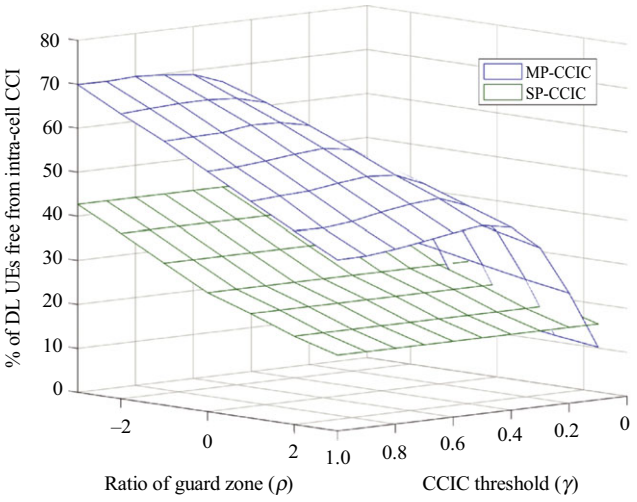

Fig. 4. Percentage of DL UEs which are free from intra-cell CCI.

in Table 1, where the radius of GZ is given by

$$R = \rho \times 40\,\text{m}, \tag{15}$$

with $0 \le \rho \le 1$ representing the GZ radius-to-pico-cell radius ratio. In addition, the length of each time slot assigned to each DL UE and UL UE pair is assumed to be the same.

This figure shows that, depending on the values of ρ and γ, the maximum 71% of DL UEs become free from the intra-cell CCI after the proposed MP-CCIC is applied, whereas the maximum 42% of DL UEs are free from the intra-cell CCI after SP-CCIC is applied. Furthermore, the percentage of DL UEs that are not affected by intra-cell CCI after the proposed MP-CCIC is applied is always larger than that after SP-CCIC is applied for all the values of ρ when $\gamma \ge 0.2$. This is because the use of GZ in the proposed MP-CCIC increases the probability that the locations of the UL and DL UEs in each pair are sufficiently close to each other such that the intra-cell CCI is cancelled by CCIC.

From the above results, it can be inferred that the proposed MP-CCIC leads to capacity enhancement compared to SP-CCIC, with an increased number of DL UEs free from intra-cell CCI.

Meanwhile, Figs. 5 and 6 show percentage increases in the average DL and sum capacities of the UD-IFD cellular network compared to the HD cellular network, respectively, when SP-CCIC and MP-CCIC are applied. For comparison, these figures also show increases in the average DL and sum capacities of a UD-IFD cellular network with no CCIC compared to an HD cellular network. The results were obtained with the same simulation setup as in Fig. 4.

These figures show that MP-CCIC improves the capacity performance of the UD-IFD cellular network

https://doi.org/10.4218/etrij.2017-0093

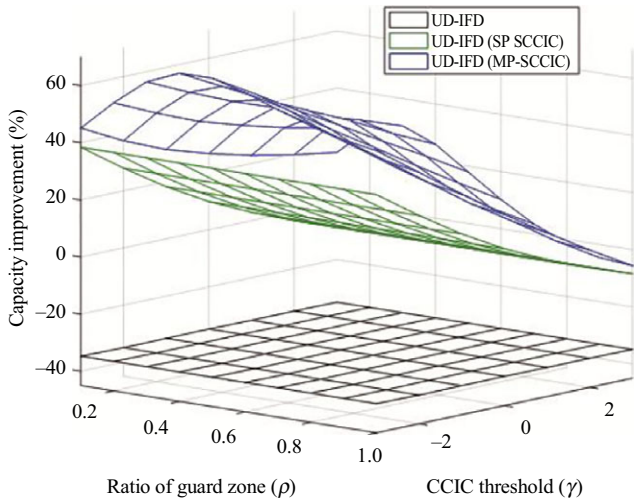

Fig. 5. Comparison of DL capacity improvement over HD.

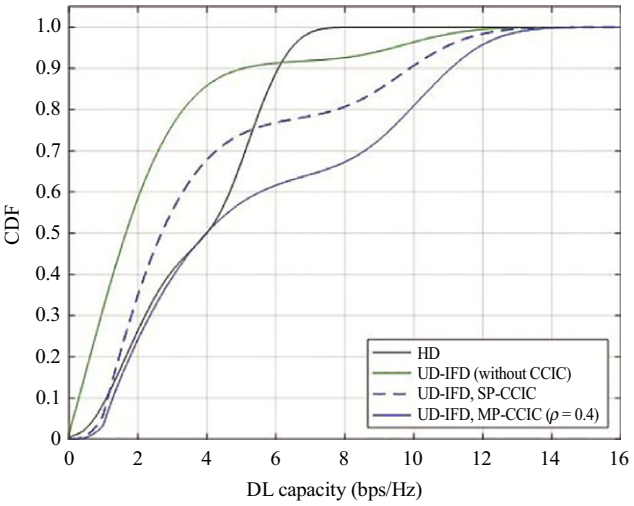

Fig. 7. Comparison of CDFs of DL capacity.

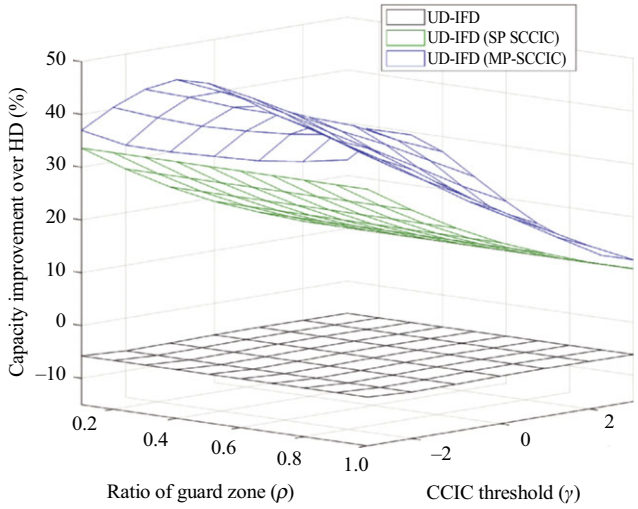

Fig. 6. Comparison of sum capacity improvement over HD.

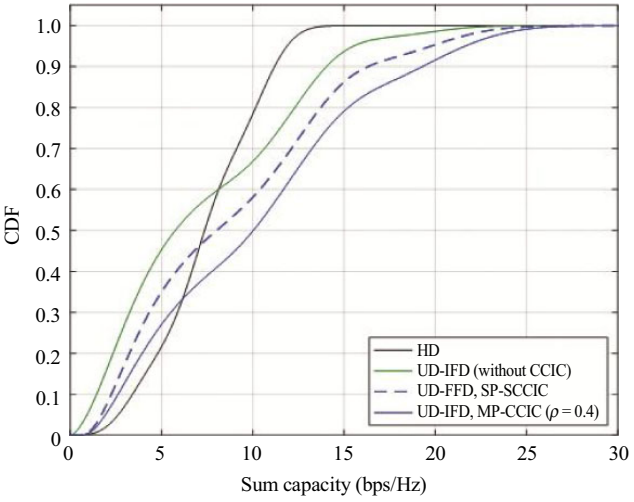

Fig. 8. Comparison of CDFs of sum capacity.

more effectively than any other techniques. When γ is -3 dB, 0 dB, and 3 dB, in particular, the DL capacity of the UD-IFD cellular network with MP-CCIC is improved 70%, 47%, and 30% over that of the HD cellular network, respectively, whereas the sum capacity is improved 50%, 38%, and 30%. In addition, it can be observed that the DL and sum capacities of the UD-IFD cellular network with the proposed MP-CCIC first increase with ρ, and then decrease with an increasing ρ for a given value of γ. This is because the probability of a DL UE being paired with a UL UE that is located in the GZ of the DL UE is too small when the value of ρ is too small. However, this probability increases as the value of ρ increases. Therefore, the probability of removing the intra-cell CCI through MP-CCIC also increases, which leads to an increase in the capacity performance. If the value of ρ becomes larger than a certain value, however, the distance between the paired DL UE and UL UE is more likely to become too large to apply MP-CCIC, although the UL UE is in the GZ of the DL UE paired with it. This is because the received power of the intra-cell CCI at the DL UL is not sufficiently large for decoding. This results in a decrease in the probability of MP-CCIC being applied, leading to a degraded capacity.

From the above results, it can be inferred that the capacity of a UD-IFD cellular network using the proposed MP-CCIC can be optimized by properly selecting the size of the GZ according to the CCIC capability of DL UEs.

Next, Figs. 7 and 8 show the CDFs of the DL and the sum capacities of various UD-IFD cellular networks (without CCIC, with SP-CCIC, and with MP-CCIC), respectively, to evaluate the effect of employing CCIC.

For a UD-IFD cellular network with SP-CCIC and MP-CCIC, it is assumed that γ = 0 dB. For the case with MP-CCIC, ρ is set to 0.4 to maximize both the DL and sum capacities in accordance with Figs. 4 and 5. Finally, for comparison, the CDFs of the DL and sum capacities of an HD cellular network are also included.

As observed in these figures, CCIC is effective for a capacity enhancement of the UD-IFD network. In particular, MP-CCIC is more effective for capacity enhancement than SP-CCIC. Compared to the HD cellular network, MP-CCIC improves the DL capacity of the IFD cellular network from even low-capacity to high-capacity regimes, whereas cases without CCIC and with SP-CCIC are rather degraded in a low-capacity regime. Note that the improvement in the DL capacity with MP-CCIC is more prominent than that of the sum capacity. This is because, by applying the MP-CCIC, the DL capacity of the UD-IFD cellular network is improved to be larger than the UL capacity and the DL capacity no longer deteriorates the sum capacity.

V. Conclusion

In this paper, we analyzed the capacity of a UD-IFD cellular network through simulations based on a 3GPP simulation methodology, and we proposed MP-CCIC method for a DL to improve the capacity. Simulation results showed that, without using CCIC, the IFD application could not yield a capacity gain in the UD-IFD cellular network compared to the HD cellular network. Even with SP-CCIC, it was observed that a sufficient capacity gain was not achieved in the UD-IFD cellular network. On the other hand, by optimally selecting the GZ size, the capacity performance of the UD-IFD cellular network using the proposed MP-CCIC was greatly improved compared with that of the HD cellular network.

The proposed MP-CCIC can be further optimized through the application of various criteria, such as the minimum rate requirement of users, fairness between users, and traffic asymmetry considerations. Moreover, an ideal CCIC was assumed in this study, which completely removes CCI under certain conditions. It is thus necessary to develop practical CCIC schemes and related technologies that achieve the performance of this ideal CCIC. The above aspects remain our future work.

Acknowledgements

This work was partly supported by ‘The Institute for Information and Communications Technology Promotion (IITP) grant’ (No. 2014-0-00282, Development of 5G Mobile Communication Technologies for Hyper-Connected Smart Services) and ‘The Cross-Ministry Giga KOREA Project’ grant (No. GK17N0100, 5G Mobile Communication System Development based on mmWave), both funded by the Korean government (MSIT).

References

[1] D. Bharadia, E. Mcmilin, and S. Katti, “Full Duplex Radios,” *Proc. ACM Special Interest Group Data Commun. (SIGCOMM)*, Hong Kong, China, Aug. 12–16, 2013, pp. 375–386.

[2] M. Chun et al., “Prototyping Real-Time Full Duplex Radios,” *IEEE Commun. Mag.*, vol. 53, no. 9, Sept. 2015, pp. 56–63.

[3] H. Ju et al., “Novel Digital Cancellation Method in the Presence of Harmonic Self-Interference,” *ETRI J.*, vol. 39, no. 2, Apr. 2017, pp. 245–254.

[4] V. Tapio and M. Sonki, “Analog and Digital Self-Interference Cancellation for Full-Duplex Transceiver,” *Proc. IEEE Eur. Wireless Conf.*, Oulu, Finland, May 18–20, 2012, pp. 1–5.

[5] D. Kim, H. Lee, and D. Hong, “A Survey of In-band Full-Duplex Transmission: From the Perspective of PHY and MAC Layers,” *IEEE Commun. Survey Tutor.*, vol. 17, no. 4, Oct. 2015, pp. 2017–2046.

[6] H. Ju et al., “Bi-Directional Beamforming and Its Capacity Scaling in Pairwise Two-Way Communications,” *IEEE Trans. Wireless Commun.*, vol. 11, no. 1, Jan. 2012, pp. 346–357.

[7] S. Wang, V. Wenkateswaran, and X. Zhang, “Exploring Full-Duplex Gains in Multi-cell Wireless Networks: A Spatial Stochastic Framework,” *Proc. IEEE Conf. Comput. Commun. (INFOCOM)*, Hong Kong, China, Apr. 26–May 1, 2015, pp. 855–863.

[8] X. Wang, H. Huang, and T. Hwang, “On the Capacity Gain from Full Duplex Communications in a Large Scale Wireless Networks,” *IEEE Trans. Mobile Comput.*, vol. 15, no. 9, Sept. 2016, pp. 2290–2303.

[9] Z. Tong and M. Haenggi, “Throughput Analysis for Full-Duplex Wireless Networks with Imperfect Self-Interference Cancellation,” *IEEE Trans. Commun.*, vol. 63, no. 11, Nov. 2015, pp. 4490–4500.

[10] S. Goyal et al., “Full Duplex Cellular Systems: Will Doubling Interference Prevent Doubling Capacity?” *IEEE Commun. Mag.*, vol. 53, no. 5, 2015, pp. 121–127.

[11] M. Duarte, A. Feki, and S. Calentin, “Inter-User Interference Coordination in Full-Duplex Systems Based on Geographical Context Information,” *Proc. IEEE Int. Conf. Commun. (ICC)*, Kuala Lumpur, Malaysia, May 2016, pp. 1–7.

[12] M.A. Khofastepour et al., "Exploring the Potential for Full Duplex in Legacy LTE Systems," *Proc. IEEE Int. Conf. Sensing, Commun. Network. (SECON)*, Singapore, June 2014, pp. 10–18.
[13] M. Mohammadi et al., "Full-Duplex Radio for Uplink/Downlink Wireless Access with Spatially Random Nodes," *IEEE Trans. Commun.*, vol. 63, no. 12, Dec. 2015, pp. 5250–5266.
[14] J. Bai and A. Sabharwal, "Distributed Full-Duplex Via Wireless Side-Channels: Bounds and Protocols," *IEEE Trans. Wireless Commun.*, vol. 12, no. 8, Aug. 2013, pp. 4162–4173.
[15] A. Sahai, S. Diggavi, and A. Sabharwal, "On Degrees-of-Freedom of Full-Duplex Uplink/Downlink Channel," *Proc. IEEE Inform. Theory Workshop (ITW)*, Seville, Spain, Dec. 2013, pp. 1–5.
[16] G. Yu, D. Wen, and F. Qu, "Joint User Scheduling and Channel Allocation for Cellular Networks with Full Duplex Base Stations," *IET Commun.*, vol. 10, no. 5, Mar. 2016, pp. 479–486.
[17] Y. Xin et al., "Co-channel Interference Suppression Techniques for Full Duplex Cellular Networks," *China Commun.*, vol. 12, Dec. 2015, pp. 18–27.
[18] 3GPP TR 36.828, "Further Enhancements to LTE Time Division Duplex (TDD) for Downlink-Uplink (DL-UL) Interference Management and Traffic Adaptation," vol. 11.0.0, June 2012.
[19] X. Zhang and M. Haenggi, "The Performance of Successive Interference Cancellation in Random Wireless Networks," *IEEE Trans. Inform. Theory*, vol. 60, no. 10, Oct. 2014, pp. 6368–6388.

Hyungsik Ju received BS and PhD degrees in electrical engineering from Yonsei University, Seoul, Rep. of Korea, in 2005 and 2011, respectively. From September 2011 to March 2012, he was a researcher at Yonsei University. From March 2012 to August 2014, he was a research fellow at the Department of Electrical and Computer Engineering of the National University of Singapore. Since 2014, he has been a senior researcher at the ETRI, Daejeon, Rep. of Korea. His research interests include full-duplex wireless communication, wireless information and power transfer, wireless-powered networks, relay-based multi-hop communication, and full-duplex relay systems.

Donghyuk Gwak received BS and MS degrees in electrical engineering from Seoul National University, Rep. of Korea, in 2010 and 2013, respectively. Since 2013, he has been a researcher at the ETRI, Daejeon, Rep. of Korea. His interests include beamforming, interference management, compressive sensing, and massive MIMO.

Sun-Ae Kim received BS and PhD degrees from Chungbuk National University, Cheong-ju, Rep. of Korea, in 2005 and 2011, respectively. Since September 2011, she has been a senior researcher at the ETRI, Daejeon, Rep. of Korea. Her research interests include full duplex wireless communication, beamforming, and D2D communication.

Yuro Lee received BS and MS degrees in electrical engineering from Seoul City University, Rep. of Korea, in 1997 and 1999, respectively. Since 2001, he has been a principal research engineer with the ETRI, Daejeon, Rep. of Korea. His research interests include broadband wireless transmission technologies and 5G mobile communications.

Tae-Joong Kim received BS, MS, and PhD degrees from Yonsei University, Seoul, Rep. of Korea, in 1991, 1993, and 1998, respectively. From 1998 to 2000, he was a senior researcher at the ETRI, Daejeon, Rep. of Korea. He joined Eonex, Ltd., in 2001, where he worked in chipset system design and later in software protocol stacks and field testing until 2006. He returned to the ETRI in 2006 and developed the 4G-LTE and 5G mobile communication systems. He is currently the managing director of the ETRI Mobile Transmission Research Department, where he manages government-sponsored 5G projects.